Online ISSN 1848-3380, Print ISSN 0005-1144
ATKAFF 57(4), 968–981(2016)

Padideh Rasouli, Khoshnam Shojaei, Abbas Chatraei

Output Feedback Look-ahead Position Control of Electrically Driven Fast Surface Vessels

DOI 10.7305/automatika.2017.12.1485
UDK [681.532.8.037-55:681.587]:629.585-83

Original scientific paper

Robust tracking control is of great importance for the surface vessels applications. This paper addresses the design of a trajectory tracking controller for fast underactuated ships in the presence of model uncertainties without velocity measurements in the yaw and surge directions. An observer-based trajectory tracking controller is proposed for the fast underactuated ship model. Then, the dynamic surface control approach is effectively exploited to propose a tracking controller considering the actuator dynamics. An adaptive robust controller is also used to compensate both the parametric and non-parametric uncertainties in the fast underactuated ship model. A Lyapunov-based stability analysis is utilised to guarantee that tracking and state estimation errors are uniformly ultimately bounded. Simulation results are presented to illustrate the feasibility and efficiency of the proposed controller.

Key words: Actuator dynamics, adaptive control, model uncertainty, output feedback, trajectory tracking.

Upravljanje pozicijom električki pokretanog brzog površinskog vozila korištenjem unaprijedne projekcije izlazne povratne veze. Robusno praćenje je pitanje od velikog praktičnog značaja za površinska vozila. Ovaj se rad bavi projektiranjem regulatora za praćenje trajektorije za brze podaktuirane brodove s modelima nesigurnosti bez mjerenja brzine u smjerovima zaošijanja i uzdužnog napredovanja. Regulator za praćenje putanje zasnovan na observeru predložen je za brz podaktuiran model broda. Upravljanje površinskom dinamikom je učinkovito iskorišteno kako bi se predložio regulatora za praćenje trajektorije s obzirom na dinamiku aktuatora. Također su primjenjene adaptivne robusne tehnike kako bi se nosile sa parametrijskim i neparametrijskim nesigurnostima u modelu brzog podaktuiranoga broda. Analiza stabilnosti temeljena na Lyapunovu se koristi kako bi se zajamčilo da su pogreške praćenja i estimacije stanja Adaptivni robusni regulator također se koristi kako bi kompenzirao parametarske i neparametarske nesigurnosti u brzom podaktuiranom brodskom modelu. Analiza stabilnosti temeljena na Lyapunovu se koristi kako bi se zajamčilo da su pogreške praćenja i procjene stanja jednoliko konačno ograničene. Prikazani su simulacijski rezultati koji ilustriraju izvedivost i učinkovitost predloženog regulatora.

Ključne riječi: Dinamika aktuatora, adaptivno upravljanje, model nesigurnosti, izlazna povratna veza, praćenje trajektorije

1 INTRODUCTION

The motion control of underactuated surface vessels has attracted a great deal of attention from the control and ocean engineering communities over the past years due to the important applications of such systems in transportation, environmental surveying and offshore installations. An important motion control problem is the trajectory tracking which is involved in the design of a controller to force a vessel to track a geometric path with associated timing law [1]. Ship control problems are challenging due to the fact that the motion of underactuated surface vessels posses more degrees of freedom to be controlled than the number of independent inputs under nonintegrable second order non-holonomic constraints [2]. In particular, only surge force and yaw moment are available in such vessels whereas there are three degrees of freedom (yaw, sway and surge direction). Since, the ships in question do not meet Brocket theorem [3], there isn't any time invariant feedback control law for asymptotical stabilizing the ship dynamics. Motivated by the challenging nature of the problems and numerous practical applications of the ships, many researchers proposed various controllers to solve the trajectory tracking and path following problems of underactuated ships [4-25].

Many of the previous works has been widely used backstepping technique. However, explosion of complexity because of repeated differentiations of virtual controllers in the design procedure, is a drawback of this tech-

nique. In [6], two control laws based on Lyapunov's direct method and combined cascade-backstepping approach are designed under a sufficient condition for persistent excitation. The work in [6] is improved and a robust control law is developed in [9]. A controller based on backstepping technique is proposed in [12] to tackle both stabilisation and tracking problems, under constant disturbances. To eliminate the aforementioned problem of backstepping technique, DSC (dynamic surface control) is employed in [22] and a controller is proposed which is much simpler than the backstepping-based controllers. However, uncertainties are ignored in this work. The reader is referred to [26] for DSC technique.

In practice, ships are usually not equipped with the velocity sensor. Therefore, estimates of the velocities are essential for feedback control. Since, the position measurements are corrupted by noise, differentiation of the position to obtain the velocities is not effective. So, an observer should be used to get the velocities. However, designing an observer-based output feedback trajectory tracking control of ships is a challenging task due to the existence of unmeasured velocities in the ship dynamics (especially in the coriolis matrix). Also, the underactuation of these vessels makes the design of the output feedback controller more challenging. In [23], a global output feedback tracking controller was proposed based on backstepping technique. It is shown that the tracking errors are globally asymptotically converge to a ball containing the origin. But, the system loses its stability in the presence of large disturbances. Also, the parametric uncertainties and model uncertainties are ignored in this work. By transforming the inertia matrix into a symmetric form, two adaptive controllers (a full-state feedback controller and an output feedback controller) in the presence of parametric uncertainties are proposed in [24]. However, non-parametric uncertainties are ignored in the design of the controller. In [25], by applying sampled-data control theory based on the Euler approximate model, a state feedback controller and reduced-order observer are designed. Then, an output feedback discrete time controller is obtained by combining the controller and observer. However, this work does not consider uncertainties or disturbances in the design of the controller.

In this paper, motivated by [27], we address the difficulties in designing the output feedback controller for trajectory tracking of underactuated fast ships including actuator dynamics and in the presence of uncertainties. The DSC methodology and adaptive robust techniques in conjunction with a linear observer are employed to design an output feedback tracking control system. The main contributions of the paper are listed as follows: (i) This is the first attempt for the development of an adaptive robust controller for fast underactuated ships including actuator dynamics, which does not require velocity measurements; (ii) In contrast to [23-25] all types of uncertainties are considered in the design of the controller. The adaptive robust controller is designed such that it estimates the unknown constants of an upper bounding function of the lumped uncertainty because of unknown parameters of the system, external disturbances and unmodelled dynamics; (iii) in contrast to previous output feedback controllers [23, 24], the proposed controller has a simpler structure and does not require any transformation matrix in the design of the controller. A Lyapunov-based stability analysis shows that all signals in the closed-loop system are uniformly ultimately bounded (UUB) and converge to a small ball centered at the origin.

The remainder of the paper is arranged as follows. The problem formulation is presented in the next section. Development of the tracking controller and Lyapunov-based stability analysis of the closed-loop control system are given in section 3. In section 4, simulation results are provided to evaluate the effectiveness of the proposed controller. Conclusions are given in section 5.

2 PROBLEM FORMULATION

Notations Throughout this paper, $\lambda_{\max}(\bullet)$ ($\lambda_{\min}(\bullet)$) denotes the largest (smallest) eignevalue of a matrix. $\|x\| := \sqrt{x^T x}$ is used as Euclidean norm of a vector $x \in \Re^n$ while the norm of a matrix A is defined as the induced norm $\|A\| := \sqrt{\lambda_{\max}(A^T A)}$, the matrix I_n denotes n-dimensional identity matrix, $Blkdiag\{\bullet\}$ shows block-diagonal form of matrices.

2.1 Kinematics and Dynamics of Underactuated Ships

Consider a class of underactuated ships whose mathematical model in a horizontal plane is described as follows [29]:

$$\begin{aligned} \dot{x} &= u\cos\psi - v\sin\psi, \\ \dot{y} &= u\sin\psi + v\cos\psi, \\ \dot{\psi} &= r, \end{aligned} \tag{1}$$

$$\begin{aligned} \dot{u} &= \tfrac{m_{22}}{m_{11}} vr - \tfrac{d_{11}}{m_{11}} u + \tfrac{1}{m_{11}}\tau_u + \tfrac{1}{m_{11}}\tau_{wu}(t), \\ \dot{v} &= -\tfrac{m_{11}}{m_{22}} ur - \tfrac{d_{22}}{m_{22}} v + \tfrac{1}{m_{22}}\tau_{wv}(t), \\ \dot{r} &= \tfrac{m_{11}-m_{22}}{m_{33}} uv - \tfrac{d_{33}}{m_{33}} r + \tfrac{1}{m_{33}}\tau_r + \tfrac{1}{m_{33}}\tau_{wr}(t), \end{aligned} \tag{2}$$

where $\eta = [x,\, y,\, \psi]^T$ denotes the position, i.e. surge and sway displacements, and orientation, i.e. the yaw angle with coordinates in the earth-fixed frame of the ship, the vector $V = [u,\, v,\, r]^T$ represents the surge, sway and angular velocities in the body-fixed frame, and the positive constant terms $d_{ii} > 0$ and $m_{ii} > 0, 1 \le i \le 3$ denote the hydrodynamic damping and ship inertia including added mass in surge, sway and yaw, and τ_u and τ_r denote required force and torque which are provided by the actuators, $\tau_{wu}(t),\ \tau_{wv}(t),\ \tau_{wr}(t) \in \Re$ are constants and time-varing bounded disturbances. The kinematic model (1) can

be expressed as follows:

$$\dot{\eta} = S(\psi)\upsilon + \delta(v, \psi). \tag{3}$$

where $\upsilon = [u, r]^T$ is a new velocity vector in the surge and yaw directions, and $\delta(v, \psi) \in \Re^3$ denotes a vector of unmatched disturbance as follows

$$S(\psi) = \begin{bmatrix} \cos\psi & 0 \\ \sin\psi & 0 \\ 0 & 1 \end{bmatrix}, \ \delta(v, \psi) = \begin{bmatrix} -v\sin\psi \\ v\cos\psi \\ 0 \end{bmatrix}. \tag{4}$$

Because we have focused on designing a controller for underactuated ship with only surge force and yaw moment available, we considered the actuated dynamics of the vessel as follows:

$$M_1\dot{\upsilon} + C_1(\upsilon)\upsilon + D_1\upsilon - \tau_{w1}(t) = \tau_a, \tag{5}$$

where M_1 is a symmetric positive-definite matrix, $C_1(\upsilon)$ is the centripetal and coriolis matrix, D_1 is the hydrodynamic damping matrix which is real and strictly positive, i.e., $D_1 > 0, \tau_{w1}(t)$ is the vector of forces and moments induced by environmental disturbances, $\tau_a = [\tau_u, \tau_r]^T$ is the vector of actuators inputs, such that

$$M_1 = \begin{bmatrix} m_{11} & 0 \\ 0 & m_{33} \end{bmatrix}, C_1(v) = \begin{bmatrix} 0 & -m_{22}v \\ (m_{22} - m_{11})v & 0 \end{bmatrix},$$
$$D_1 = \begin{bmatrix} d_{11} & 0 \\ 0 & d_{33} \end{bmatrix}, \tau_{w1}(t) = \begin{bmatrix} \tau_{wu}(t) \\ \tau_{wr}(t) \end{bmatrix}. \tag{6}$$

Property 1 M_1 is a symmetric and positive-definite matrix, i.e., $M_1 = M_1^T > 0$ which is upper and lower bounded such that $\lambda_{m_1}\|x\|^2 \leq x^T M_1 x \leq \lambda_{M_1}\|x\|^2 \ \forall x \in \Re^2$, and $0 < \lambda_{m_1} \leq \lambda_{M_1} < \infty$ where $\lambda_{m_1} := \lambda_{\min}(M_1)$ and $\lambda_{M_1} := \lambda_{\max}(M_1)$.

Property 2 The following upper-bounding functions are valid for the presented kinematic and dynamic model of the system:

$$\|S(\psi)\| \leq s_1, \|C_1(\upsilon)\| \leq \lambda_{C_1}\|\upsilon\|, \quad \|D_1\| \leq \lambda_{D_1}, \|\tau_{w_1}(t)\| \leq \lambda_{W_1}, \tag{7}$$

where $s_1, \lambda_{C_1}, \lambda_{D_1}$ and λ_{W_1} are positive scalar constants. It should be noted that the sway velocity is bounded which is stated in the sequel.

2.2 Actuator Dynamics

To take the actuator dynamics into account, it is assumed that the vessel is actuated by two brushed DC motors with mechanical gears. The drive system is shown by Fig. 1. The electrical equation of i-th motor armature is written as follows:

$$u_{ai} = l_{ai}\dot{I}_{ai} + r_{ai}I_{ai} + k_{bi}\dot{\theta}_{mi} + u_{di}, \quad \tau_{mi} = k_{\tau i}I_{ai}, \tag{8}$$

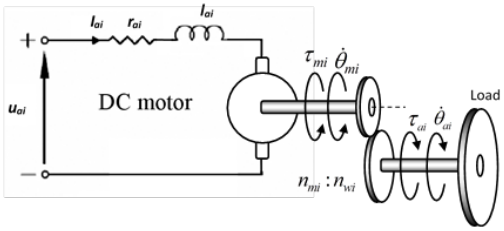

Fig. 1. Drive system for the actuation of an underactuated fast surface vessel.

where k_{bi} is the back EMF constant, r_{ai}, l_{ai} and I_{ai} denote the resistance, inductance and current of the motor armature, respectively, u_{ai} is the voltage input, u_{di} denotes the unstructured uncertainties and τ_{mi} denotes the torque which is generated by the actuators in the actuator model. By considering the relation between the torque and velocities before and after gears, i.e. $\dot{\theta}_{mi} = n_i\dot{\theta}_{ai}$ and $\tau_{ai} = n_i\tau_{mi}$, where n_i is the gear ratio, the actuators dynamics are given by

$$L_a\dot{I}_a + R_aI_a + NK_bX\upsilon + u_d = u_a. \tag{9}$$

$$\tau_a = NK_TI_a, \tag{10}$$

where $L_a = \text{diag}[l_{a1}, l_{a2}]$, $R_a = \text{diag}[r_{a1}, r_{a2}]$, $N = \text{diag}[n_1, n_2]$, $K_b = \text{diag}[k_{b1}, k_{b2}]$, $K_T = \text{diag}[k_{\tau 1}, k_{\tau 2}]$, and $\tau_a,\ u_a,\ I_a \in \Re^2$ denote the torque, voltage and armature current input vectors, respectively, and X is a transformation matrix which transforms propellers angular velocities to surge and yaw velocities. The interested reader refers to [34] for more details.

2.3 Reduced Model of Surface Vessel

For the controller design purposes, it is assumed that there exists the following smooth output equation

$$z = h(\eta) = [x + L\cos\psi, y + L\sin\psi], \tag{11}$$

where $z \in \Re^2$ is a new position variable, L is a look-ahead distance which is shown in Fig. 2. This figure shows the planar configuration of a surface vessel with two propellers. The point O_b is the origin of the body-fixed frame that is attached to the ship body. The point P_L is a virtual reference point on x-axis of the body-fixed frame at a distance L of O_b. By differentiating the output equation (11) and substituting (3), one gets:

$$\dot{z} = J(\psi)\upsilon + J_\delta(v, \psi), \tag{12}$$

where $J(\psi) = J_h(\psi)S(\psi) \in \Re^{2\times 2}$, $J_h(\psi) := \partial h(\eta)/\partial\eta$ is the Jacobain matrix and $J_\delta(v, \psi) = J_h(\psi)\delta(v, \psi)$ are

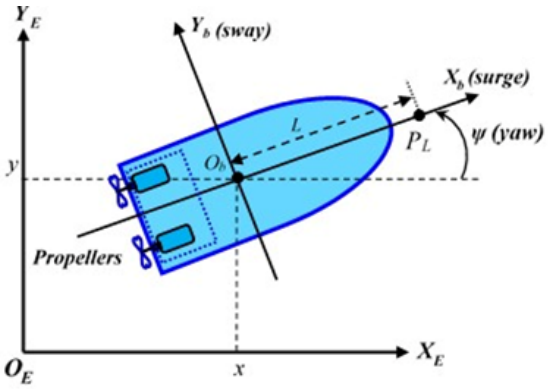

Fig. 2. Planar model of a surface vessel.

given by

$$J(\psi) = \begin{bmatrix} \cos(\psi) & -L\sin(\psi) \\ \sin(\psi) & L\cos(\psi) \end{bmatrix}, \quad (13)$$
$$J_\delta(v,\psi) = \begin{bmatrix} -v\sin(\psi) \\ v\cos(\psi) \end{bmatrix}.$$

By considering (13), the matrix $J(\psi)$ is invertible, i.e.,

$$J^{-1}(\psi) = \begin{bmatrix} \cos(\psi) & \sin(\psi) \\ -\sin(\psi)/L & \cos(\psi)/L \end{bmatrix}. \quad (14)$$

Then, one may write

$$\upsilon = J^{-1}(\psi)(\dot{z} - J_\delta(v,\psi)), \quad (15)$$

$$\begin{aligned} \dot{\upsilon} &= J^{-1}(\psi)[(\ddot{z} - \dot{J}_\delta(v,\psi)) - \dot{J}(\psi)J^{-1}(\psi)\,(\dot{z} - J_\delta(v,\psi))] \\ &= J^{-1}(\psi)[\ddot{z} - \dot{J}(\psi)J^{-1}(\psi)\dot{z}] + \rho(v,\psi), \end{aligned} \quad (16)$$

where

$$\rho(v,\psi) = -J^{-1}(\psi)[\dot{J}_\delta(v,\psi) - \dot{J}(\psi)J^{-1}(\psi)J_\delta(v,\psi)]. \quad (17)$$

Substituting (15) and (16) into (5) yields

$$\begin{aligned} &M_1 J^{-1}(\psi)\ddot{z} + C_1(v)J^{-1}(\psi)\dot{z} + D_1 J^{-1}(\psi)\dot{z} - M_1 J^{-1}(\psi) \times \\ &\dot{J}(\psi)J^{-1}(\psi)\dot{z} + M_1\rho(v,\psi) - C_1(v)J^{-1}(\psi)J_\delta(v,\psi) \\ &- D_1 J^{-1}(\psi)J_\delta(v,\psi) - \tau_{w1}(t) = \tau_a. \end{aligned} \quad (18)$$

Then, considering the actuator equations (9) and (10) and multiplying both sides of (18) by $J^{-T}(\psi)$ yields the following Earth-fixed representation:

$$M_2(\psi)\ddot{z} + C_2(v,\psi,\dot{z})\dot{z} + D_2(\psi)\dot{z} + \tau_{w2}(v,\psi,t) = J^{-T}(\psi)I_a, \quad (19)$$

where

$$\begin{aligned} M_2(\psi) &= (NK_T)^{-1}J^{-T}(\psi)M_1\,J^{-1}(\psi), \\ C_2(v,\psi,\dot{z}) &= (NK_T)^{-1}J^{-T}(\psi)\,[C_1(v) \\ &\quad - M_1 J^{-1}(\psi)\dot{J}(\psi)\big]\,J^{-1}(\psi), \\ D_2(\psi) &= (NK_T)^{-1}J^{-T}(\psi)D_1\,J^{-1}(\psi), \\ \tau_{w2}(v,\psi,t) &= (NK_T)^{-1}J^{-T}(\psi)[M_1\rho(v,\psi) \\ &\quad - C_1(v)J^{-1}(\psi)J_\delta(v,\psi) \\ &\quad - D_1 J^{-1}(\psi)J_\delta(v,\psi) - \tau_{w1}(t)]. \end{aligned} \quad (20)$$

The model (19) represents a reduced formulation of underactuated surface vessel that are denoted by (2) and (3).

Property 3 $M_2(\psi)$ is a symmetric and positive-definite matrix which is upper and lower bounded such that $\lambda_{m_2}\|x\|^2 \le x^T M_2 x \le \lambda_{M_2}\|x\|^2\ \forall x \in \Re^2$ and $0 < \lambda_{m_2} \le \lambda_{M_2} < \infty$, where $\lambda_{m_2} := \min_{\forall\psi\in\Re} \lambda_{\min}(M_2(\psi))$ and $\lambda_{M_2} := \max_{\forall\psi\in\Re} \lambda_{\max}(M_2(\psi))$.

Property 4 The matrix $\dot{M}_2(\psi) - 2\,C_2(v,\psi,\dot{z})$ is skew symmetric, i.e.,

$$x^T(\dot{M}_2(\psi) - 2\,C_2(v,\psi,\dot{z}))x = 0, \ \ \forall\, x \in \Re^2. \quad (21)$$

Property 5 There exist positive scalar constants $\lambda_{M_2}, \lambda_{C_2}, \lambda_{D_2}, \lambda_J, \lambda_{J\delta}$ and λ_{W_2} such that

$$\begin{aligned} &\|M_2(\psi)\| \le \lambda_{M2}\,, \|C_2(v,\psi,\dot{z})\| \le \lambda_{C_2}\,\|\dot{z}\|\,, \\ &\|D_2(\psi)\| \le \lambda_{D_2}\,, \|\tau_{w2}(v,\psi,t)\| \le \lambda_{W_2}, \\ &\|J(\psi)\| \le \lambda_J\,, \|J_\delta(v,\psi)\| \le \lambda_{J\delta}. \end{aligned} \quad (22)$$

2.4 Definitions and assumptions

The following tracking problem is addressed in this paper:

Definition 1 [28]. Consider the non-linear system $\dot{x} = f(x,u)$ and $z = h(x)$, where x is a state vector, u is the input vector and z is the output vector. The solution is UUB if there exists $\beta > 0$ and $\gamma > 0$, and for every $\alpha \in (0,\gamma)$ there exists a positive constant such that $\|x(t_0)\| < \alpha \Rightarrow \|x(t)\| \le \beta, \forall t \ge t_0 + T$.

Considering this definition, the following tracking problem is addressed in this paper.

Definition 2 Given a smooth bounded desired trajectory $z_d(t) = h(\eta_d(t)) : [0,\infty) \to \Re^2$ which is generated by an associated timing law, the control objective discussed in this paper is to design a feedback control law for the systems (19) such that (i) it makes the tracking errors, $z_e(t) := z(t) - z_d(t)$, be uniformly ultimately bounded in the presence of structured and unstructured uncertainties; (ii) it does not require measurements of the velocity signals; and (iii) it takes the actuator dynamics into account.

The following assumptions are essential to meet the control objectives of this paper:

Assumption 1 Measurements of output vector $z \in \Re^2$ and current I_a are available in real-time.

Assumption 2 The desired trajectory $z_d(t)$ is chosen such that $z_d(t), \dot{z}_d(t), \ddot{z}_d(t)$ and $\dddot{z}_d$ are all bounded signals in the sense that $\sup_{t\geq 0}\|z_d\| < B_{dp}, \sup_{t\geq 0}\|\dot{z}_d\| < B_{dv}, \sup_{t\geq 0}\|\ddot{z}_d\| < B_{da}$ and $\sup_{t\geq 0}\|\dddot{z}_d\| < B_{dj}$ where B_{dp}, B_{dv}, B_{da} and B_{dj} are bounded constants.

Assumption 3 In (1), the sway velocity v is passive-bounded in sense that $\sup_{t\geq 0}\|v(t)\| < B_v$. However, in most practical applications of the surface vessels [29], it is not difficult to verify that this assumption is always satisfied. For more details, see [30].

3 OUTPUT FEEDBACK CONTROL DESIGN

In this section, to achieve the control objective, an output feedback trajectory tracking controller is designed using the DSC method. Then, a Lyapunov-based stability analysis is applied to prove that the tracking errors and state estimation errors are UUB.

3.1 Recursive controller-observer design

Step1: Consider the following definitions

$$\dot{z}_r := \dot{z}_d - \Lambda(\hat{z} - z_d) = \dot{z}_d - \Lambda z_e + \Lambda z_z, \tag{23}$$

$$\dot{z}_o := \dot{\hat{z}} - \Lambda z_z, \tag{24}$$

$$r := \dot{z} - \dot{z}_o = \dot{z}_z + \Lambda z_z, \tag{25}$$

where $z_z := z - \hat{z}$ is the observation error vector, $\Lambda \in \Re^{2\times 2}$ denotes a diagonal positive- definite gain matrix. Considering the above definitions, the first dynamic surface is defined as

$$S_1 := \dot{z} - \dot{z}_r = \dot{z}_e + \Lambda z_e - \Lambda z_z. \tag{26}$$

Considering (19) and applying (26) yield

$$M_2(\psi)\dot{S}_1 = -C_2(v,\psi,\dot{z})S_1 - D_2(\psi)S_1 + \xi + J^{-T}(\psi)I_a, \tag{27}$$

where $\xi = -M_2(\psi)\ddot{z}_r - C_2(v,\psi,\dot{z})\dot{z}_r - D_2(\psi)\dot{z}_r - \tau_{w2}(v,\psi,t)$ denotes the uncertain non-linearities which are bounded as $\|\xi\| \leq f(\dot{z}_r, \ddot{z}_r)$ by using property (5). We now choose $\bar{I}_a$ to make $S_1 \to 0$, the following adaptive robust virtual tracking controller is proposed

$$\begin{aligned}\bar{I}_a = J^T(\psi)(&-K_1(\dot{z}_o - \dot{z}_r) - K_2(z_e + z_z)\\ &-f_c(\hat{f}(\dot{z}_r, \ddot{z}_r)\operatorname{sign}(S_1 + r)))\,,\end{aligned} \tag{28}$$

where K_1 and $K_2 \in \Re^{2\times 2}$ are positive-definite diagonal gain matrices. The control term f_c is a continuous approximation of Signum function, which satisfies the following conditions [31]:

$$(S_1 + r)^T f_c(\hat{f}\operatorname{sign}(S_1 + r)) \geq 0, \tag{29}$$

$$\hat{f}\,\|S_1 + r\| - (S_1 + r)^T f_c(\hat{f}\operatorname{sign}(S_1 + r)) \leq \delta_1(t) + \delta_2(t),$$

where $\delta_i(t),\ i = 1, 2$ are bounded time-varying positive scalars. In the control law (28), $\hat{f}(\dot{z}_r, \ddot{z}_r) = F(\dot{z}_r, \ddot{z}_r)\hat{\alpha}$ is the estimate of the upper-bounding function $f(\dot{z}_r, \ddot{z}_r)$, where $F(\dot{z}_r, \ddot{z}_r) = \left[\begin{array}{cccc} 1 & \|\dot{z}_r\| & \|\dot{z}_r\|^2 & \|\ddot{z}_r\| \end{array}\right]$ and $\hat{\alpha}$ is updated by

$$\dot{\hat{\alpha}} = \Gamma_1 F^T(\dot{z}_r, \ddot{z}_r)\,\|S_1 + r\| - \Gamma_1\sigma_1(\hat{\alpha} - \alpha_0), \tag{30}$$

where $\Gamma_1 = \gamma_1 I_4$ denotes the adaptation gain, σ_1 is a small positive number and $\alpha_0 \in \Re^4$ is a priori estimate of the parameters. To estimate the velocity vector, the following linear observer [32] is utilized

$$\dot{\hat{z}} = \dot{\hat{z}}_o + \Lambda z_z + k_o z_z, \tag{31}$$

$$\ddot{\hat{z}}_o = \ddot{z}_r + k_o \Lambda z_z, \tag{32}$$

where k_o is a positive constant. Equation (12) can be applied to compute the velocities estimates. Then, the virtual control signal $\bar{I}_a$ is passed through the following first order filter

$$\tau\dot{I}_{af} + I_{af} = \bar{I}_a, I_{af}(0) = \bar{I}_a(0), \tag{33}$$

where I_{af} denotes the filtered virtual tracking control and τ is a positive design parameter.

Step 2: Consider the actuator dynamic (9). The second dynamic surface is defined as

$$S_2 = I_a - I_{af}. \tag{34}$$

Differentiating S_2 and substituting (9), yield

$$L_a\dot{S}_2 = L_a\dot{I}_a - L_a\dot{I}_{af} = u_a - R_a I_a - NK_bXv - u_d - L_a\dot{I}_{af}. \tag{35}$$

By applying (15) and (34) into (35), one may write

$$L_a\dot{S}_2 = u_a - R_a S_2 - NK_bXJ^{-1}\dot{z}_e + \zeta, \tag{36}$$

where

$$\zeta = -R_a I_{af} - NK_bXJ^{-1}\dot{z}_d + NK_bXJ^{-1}J_\delta - L_a\dot{I}_{af} - u_d$$

denotes the uncertain non-linearities which may be bounded as $\|\zeta\| \leq h(\dot{z}_d, I_{af}, \dot{I}_{af}) := H(\dot{z}_d, I_{af}, \dot{I}_{af})\beta$, where β is a vector of uncertain parameters and $H(\dot{z}_d, I_{af}, \dot{I}_{af}) = \left[\begin{array}{cccc} 1 & \|I_{af}\| & \left\|\dot{I}_{af}\right\| & \|\dot{z}_d\| \end{array}\right]$. Then, the actual control input is proposed as follows:

$$u_a = -K_3 S_2 - h_c(\hat{h}\operatorname{sign}(S_2)), \tag{37}$$

where $h_c \in R^2$ denotes the continuous approximation of signum function, which also satisfies the following conditions [31]

$$\begin{aligned} &S_2^T h_c(\hat{h}\operatorname{sign}(S_2)) \geq 0,\\ &\hat{h}\,\|S_2\| - S_2^T h_c(\hat{h}\operatorname{sign}(S_2)) \leq \iota_1(t) + \iota_2(t),\end{aligned} \tag{38}$$

where $\hat{h} = H\hat{\beta}$ denotes the estimated upper bounding function h and $\hat{\beta}$ is updated by

$$\dot{\hat{\beta}} = \Gamma_2 H^T \|S_2(t)\| - \Gamma_2\sigma_2(\hat{\beta} - \beta_0). \tag{39}$$

where $\Gamma_2 = \gamma_2 I_4$ denotes the adaptation gain, σ_2 is a small positive number, $\beta_0 \in \Re^4$ is a priori estimate of parameters. In (38), $\iota_i(t),\ i = 1, 2$ are bounded time-varying positive scalars. The controller (37) does not need differentiation of the virtual controller (28), since it can be computed by the first order filter (33).

3.2 Stability analysis

Following preliminaries are needed for Lyapunov stability. Define the boundary layer error as

$$e_f = I_{af} - \bar{I}_a. \tag{40}$$

By considering (28), (33) and (40), the derivative of e_f is given by

$$\dot{e}_f = \dot{I}_{af} - \dot{\bar{I}}_a = -\frac{e_f}{\tau} + \frac{\partial J^T}{\partial \psi} S(\psi) J^{-1}(\psi)\dot{z}(J^{-T}(\psi)\bar{I}_a) - \frac{\partial J^T}{\partial \psi} S(\psi) J^{-1}(\psi) J_\delta(v,\psi)(J^{-T}(\psi)\bar{I}_a) + \frac{\partial J^T}{\partial \psi}\delta(v,\psi)\times (J^{-T}(\psi)\bar{I}_a) + J^T(\psi)(K_1(\ddot{z}_o - \ddot{z}_r) + K_2(\dot{z}_e + \dot{z}_z) + \dot{f}_c). \tag{41}$$

The interested reader is referred to [33] for a continuous differentiable robust control f_c. On mat verify that all terms in (41) can be dominated by some continuous functions. This helps us to write

$$\left\| \dot{e}_f + \frac{e_f}{\tau} \right\| \le \rho(S_1, S_2, r, e_f, z_e, z_z, \hat{\alpha}, z_d, \dot{z}_d, \ddot{z}_d, \dddot{z}_d), \tag{42}$$

where ρ is a continuous function. Multiplying both sides of (42) by e_f^T, yields

$$e_f^T\dot{e}_f + \frac{1}{\tau}e_f^T e_f \le \left\| e_f^T\dot{e}_f + \frac{1}{\tau}e_f^T e_f \right\| \le \rho \|e_f\|. \tag{43}$$

As a result, we have

$$e_f^T\dot{e}_f \le -\frac{1}{\tau}e_f^T e_f + \rho\|e_f\| \le -\frac{1}{\tau}e_f^T e_f + e_f^T e_f + \frac{1}{4}\rho^2. \tag{44}$$

Then, considering that $S_1 - r = \dot{z}_o - \dot{z}_r$ and substituting (34), (40) and (28) into (27), the closed-loop system dynamics may be achieved as

$$M_2(\psi)\dot{S}_1 = -C_2(v,\psi,\dot{z})S_1 + \xi + \chi_1 + J^{-T}(\psi)(e_f + S_2) - K_1S_1 + K_1 r - K_2 z_e - K_2 z_z - f_c. \tag{45}$$

where $\chi_1 = -D_2(\psi)S_1$ which is bounded as $\|\chi_1\| \le \zeta_1\|x\| + \zeta_2\|x\|^2$ where

$$x = [z_e^T, z_z^T, S_1^T, r^T]^T. \tag{46}$$

By considering (31) and (32), one may show that $\dot{S}_1 = \dot{r} + k_o r$ which together with (45) and $S_1 - r = \dot{z}_o - \dot{z}_r$ yield the following error equation

$$M_2(\psi)\dot{r} = -C_2(v,\psi,\dot{z})r - (k_o M_2(\psi) - K_1)r - K_1S_1 - K_2 z_e - K_2 z_z - f_c + \chi_2 + \xi + J^{-T}(\psi)(e_f + S_2). \tag{47}$$

where $\chi_2 = C_2(v,\psi,S_1 + \dot{z}_r)r - C_2(v,\psi,\dot{z})S_1 - D(\psi)S_1$ which is bounded as follows:

$$\|\chi_2\| \le \zeta_3\|x\| + \zeta_4\|x\|^2. \tag{48}$$

Substituting (37) into (36) yields

$$L_a\dot{S}_2 = -K_3S_2 - R_aS_2 - NK_bXJ^{-1}\dot{z}_e + \zeta - h_c(\hat{h}\,\mathrm{sign}(S_2)). \tag{49}$$

The stability of the resulting closed-loop dynamics is summarized by the following theorem.

Theorem 1 Consider the fast underactuated ship system (19). Given a bounded continuous desired trajectory, under Assumption 1-3, the output feedback controller (28), (37), (31) and (32) with the conditions (29) and (38) and the adaptive laws (30) and (39) ensures that all signals in the closed-loop system are bounded, the tracking errors $z_e(t) = z(t) - z_d(t)$ and observation errors $z_z(t) = z(t) - \hat{z}(t)$ are UUB and exponentially converge to small ball containing the origin. Moreover, the following region of attraction can be made arbitrarily large to include any initial conditions by selecting the control gains large enough.

$$R_A = \left\{ \vartheta \in \Re^{20} \;\middle|\; \|\vartheta\| < \sqrt{\frac{2\lambda_{\min}(A^*) - (\zeta_1 + \zeta_3)}{(\zeta_2 + \zeta_4)\lambda_{\max}(P)/\lambda_{\min}(M^*)}} \right\} \tag{50}$$

where $\vartheta = [x^T, S_2^T, e_f^T, \tilde{\alpha}^T, \tilde{\beta}^T]^T$, $\lambda_{\min}(A^*)$ is a positive gain-dependent parameter, $x \in \Re^8$ was defined in (46) and matrices P and M^* will be defined later.

Proof: Consider the following Lyapunov function candidate

$$V(t) = \frac{1}{2}z_e^T K_2 z_e + \frac{1}{2}z_z^T K_2 z_z + \frac{1}{2}S_1^T M_2(\psi)S_1 + \frac{1}{2}r^T M_2(\psi)r + \frac{1}{2}S_2^T L_a S_2 + \frac{1}{2}e_f^T e_f + \frac{1}{2}\tilde{\alpha}^T\Gamma_1^{-1}\tilde{\alpha} + \frac{1}{2}\tilde{\beta}^T\Gamma_2^{-1}\tilde{\beta}. \tag{51}$$

As shown in Appendix, differentiating (51) along (25), (26), (45), (47), (49), (30) and (39), after some manipu-

lations, one can get

$$\begin{aligned}\dot{V}(t)\leq&-\lambda_{\min}(A)\|z_e\|^2-\lambda_{\min}(B)\|z_z\|^2-\lambda_{\min}(C)\|S_1\|^2\\&-\lambda_{\min}(D)\|r\|^2-\lambda_{\min}(E)\|S_2\|^2+\frac{1}{2}(\zeta_1+\zeta_3)\|x\|^2\\&+\frac{1}{2}(\zeta_2+\zeta_4)\|x\|^4-\frac{1}{\tau}e_f^Te_f+e_f^Te_f+\frac{1}{4}\rho_m^2+\\&\|\xi\|\|S_1+r\|-(S_1+r)^Tf_c+\|S_2\|\|\zeta\|-\\&S_2^Th_c+\left\|J^{-T}\right\|\|e_f\|^2-\tilde{\alpha}^TF^T||S_1+r||+\\&\tilde{\alpha}^T\sigma_1(\hat{\alpha}-\alpha_0)-\tilde{\beta}H^T||S_2||+\tilde{\beta}^T\sigma_2(\hat{\beta}-\beta_0)\,,\end{aligned}\quad(52)$$

where

$$\begin{aligned}A=&K_2\Lambda-\frac{1}{2}\|K_2\|I_2-\frac{1}{2}\left\|NK_bXJ^{-1}\Lambda\right\|I_2-\frac{1}{2}\|K_2\Lambda\|\,I_2,\\B=&K_2\Lambda-\frac{1}{2}\|K_2\|I_2-\frac{1}{2}\left\|NK_bXJ^{-1}\Lambda\right\|I_2-\frac{1}{2}\|K_2\Lambda\|\,I_2,\\C=&K_1-\frac{1}{2}(\zeta_1+\zeta_2)I_2-\left\|J^{-T}\right\|I_2-\frac{1}{2}\left\|NK_bXJ^{-1}\right\|I_2,\\D=&k_0M_2(\Psi)-K_1-\frac{1}{2}(\zeta_3+\zeta_4)I_2-\frac{1}{2}||K_2||I_2-||J^{-T}||I_2\\E=&K_3+R_a-|\!|J^{-T}|\!|I_2-\frac{1}{2}|\!|NK_bXJ^{-1}|\!|I_2-||NK_bXJ^{-1}\Lambda||I_2.\end{aligned}\quad(53)$$

Considering that $\|\xi\|\leq F\alpha$ and $\|\zeta\|\leq H\beta$, $\hat{\alpha}=\alpha-\tilde{\alpha}$, $\hat{\beta}=\beta-\tilde{\beta}$ and completing the square terms, one may write (53) as

$$\begin{aligned}\dot{V}(t)\leq&-\lambda_{\min}(A^*)\|x\|^2-\lambda_{\min}(E)\|S_2\|^2-\lambda_{\min}(F)\|e_f\|^2\\&+\frac{1}{2}(\zeta_1+\zeta_3)\|x\|^2+\frac{1}{2}(\zeta_2+\zeta_4)\|x\|^4+\frac{1}{4}\rho_m^2\\&+\|S_1+r\|F\hat{\alpha}-(S_1+r)^Tf_c-\mu_{\sigma1}(1-\frac{1}{2\kappa^2})\|\tilde{\alpha}\|^2\\&+\frac{1}{2}\mu_{\sigma1}\kappa^2\|\alpha-\alpha_0\|^2+\|S_2\|H\hat{\beta}-S_2^Th\\&-\mu_{\sigma2}(1-\frac{1}{2\kappa^2})\left\|\tilde{\beta}\right\|^2+\frac{1}{2}\mu_{\sigma2}\kappa^2\|\beta-\beta_0\|^2\,,\end{aligned}\quad(54)$$

where $A^*=Blkdiag\{A,B,C,D\}$, $\mu_{\sigma j}=\sqrt{\lambda_{\min}(\sigma_j^T\sigma_j)}$, $j=1,2$, $F=(\frac{1}{\tau}-1-\left\|J^{-T}\right\|)I_2$ and $\kappa\in\Re^+$. In (54), one can choose Λ,K_1,K_2,K_3,k_o and τ such that matrices A,B,C,D,E,F and as a result A^* are all positive definite. By applying the conditions (29) and (38) to (54), one gets

$$\begin{aligned}\dot{V}(t)\leq&-(\lambda_{\min}(A^*)-\frac{1}{2}(\zeta_1+\zeta_3)-\frac{1}{2}(\zeta_2+\zeta_4)\|x\|^2)\|x\|^2\\&-\lambda_{\min}(E)\|S_2\|^2-\lambda_{\min}(F)\|e_f\|^2\\&-\kappa_1||\tilde{\alpha}||^2-\kappa_2||\tilde{\beta}||^2+\epsilon(t)\,,\end{aligned}\quad(55)$$

where

$$\begin{aligned}\|x\|^2\leq&\lambda_{\max}(P)/\lambda_{\min}(M^*)\|\vartheta(0)\|^2\,,\\\kappa_1=&\mu_{\sigma1}(1-\frac{1}{2\kappa^2})\,,\kappa_2=\mu_{\sigma2}(1-\frac{1}{2\kappa^2}),\\\varepsilon(t)=&\frac{1}{2}\mu_{\sigma1}\kappa^2\|\alpha-\alpha_0\|^2+\frac{1}{2}\mu_{\sigma2}\kappa^2\|\beta-\beta_0\|^2\\&+\delta_1(t)+\delta_2(t)+\iota_1(t)+\iota_2(t)+\frac{1}{4}\rho_m^2,\end{aligned}\quad(56)$$

where $\vartheta=[x^T,S_2^T,e_f^T,\tilde{\alpha}^T,\tilde{\beta}^T]^T$, $M^*=Blkdiag\{K_2,\,M_2\}$ and $P=Blkdiag\{M^*,L_a,I_2,\Gamma_1^{-1},\Gamma_2^{-1}\}$. If $\lambda_{\min}(A^*)$ is chosen such that

$$\lambda_{\min}(A^*)>\frac{1}{2}(\zeta_1+\zeta_3)+\frac{1}{2}(\zeta_2+\zeta_4)\|x\|^2\,,\quad(57)$$

then, (55) can be expressed as

$$\begin{aligned}\dot{V}(t)\leq&-c_m\|x\|^2-\lambda_{\min}(E)\|S_2\|^2-\lambda_{\min}(F)\|e_f\|^2\\&-\kappa_1||\tilde{\alpha}||^2-\kappa_2||\tilde{\beta}||^2+\epsilon(t)\,,\end{aligned}\quad(58)$$

where $c_m\in\Re$ is some positive constant. On the other hand, the Lyapunov function (51) can be stated as

$$\begin{aligned}&\tfrac{1}{2}\lambda_{\min}(M^*)\|x\|^2+\tfrac{1}{2}\lambda_{\min}(L_a)\|S_2\|^2+\tfrac{1}{2}\|e_f\|^2\\&+\tfrac{1}{2}\lambda_{\min}(\Gamma_1^{-1})\|\tilde{\alpha}\|^2+\tfrac{1}{2}\lambda_{\min}(\Gamma_2^{-1})\left\|\tilde{\beta}\right\|^2\leq V(t)\leq\\&\tfrac{1}{2}\lambda_{\max}(M^*)\|x\|^2+\tfrac{1}{2}\lambda_{\max}(L_a)\|S_2\|^2\\&+\tfrac{1}{2}\|e_f\|^2+\tfrac{1}{2}\lambda_{\max}(\Gamma_1^{-1})\|\tilde{\alpha}\|^2+\tfrac{1}{2}\lambda_{\max}(\Gamma_2^{-1})\left\|\tilde{\beta}\right\|^2\\&\leq\tfrac{1}{2}\lambda_{\max}(P)\|\vartheta\|^2\end{aligned}\quad(59)$$

Then, inequality (58) is written as

$$\dot{V}(x,S_2,e_f,\tilde{\alpha},\tilde{\beta})\leq-\lambda V(x,S_2,e_f,\tilde{\alpha},\tilde{\beta})+\varepsilon(t),\quad(60)$$

where

$$\begin{aligned}\lambda=\Big\{&\tfrac{2c_m}{\lambda_{\max}(M^*)},\tfrac{2\lambda_{\min}(E)}{\lambda_{\max}(L_a)},2\lambda_{\min}(F)\\&,\tfrac{2\kappa_1}{\lambda_{\max}(\Gamma_1^{-1})},\tfrac{2\kappa_2}{\lambda_{\max}(\Gamma_2^{-1})}\Big\}.\end{aligned}\quad(61)$$

By solving the differential inequality (60), we have

$$V(t)\leq V(0)\,e^{-\lambda t}+\varepsilon/\lambda(1-e^{-\lambda t}),\forall t\in[0,\infty).\quad(62)$$

Thus, provided that matrices A,B,C,D,E and F are all positive definite and the condition (57) is satisfied, V decreases monotonically until $(x,S_2,e_f,\tilde{\alpha},\tilde{\beta})$ reaches the compact set

$$\begin{aligned}\Omega=\Big\{&(x,S_2,e_f,\tilde{\alpha},\tilde{\beta})\in\Re^{20}\times\Re:V(x,S_2,e_f,\tilde{\alpha},\tilde{\beta})\\&\leq\max\{V(t_0),\varepsilon/\lambda\}\Big\}.\end{aligned}$$

which results in the following inequality

$$V(t)\leq V(0)\leq\frac{1}{2}\lambda_{\max}(P)\|\vartheta(0)\|^2\;\forall t\geq0.\quad(63)$$

where the upper bound on $V(t)$ in (59) is used. From (63) and (59), one has

$$\|x\|^2 \leq \lambda_{\max}(P)/\lambda_{\min}(M^*)\,\|\vartheta(0)\|^2\,. \tag{64}$$

Therefore, a sufficient condition for (57) is given by

$$\begin{aligned}&\lambda_{\min}(A^*) > \tfrac{1}{2}(\zeta_1+\zeta_3)+\tfrac{1}{2}(\zeta_2+\zeta_4)\times\\&(\lambda_{\max}(P)/\lambda_{\min}(M^*)\,\|\vartheta(0)\|^2\,.\end{aligned} \tag{65}$$

This results in the region of attraction in (50). Hence, $x, S_2, e_f, \tilde{\alpha}, \tilde{\beta}$ are semi-globally uniformly ultimately bounded. This completes the proof.

Remark 1: In order to make (28) and (30) independent from velocity measurements, the term $S_1 + r$ is substituted by $\hat{S}_1 + \hat{r} =: \dot{\hat{z}} - \dot{z}_d + \Lambda z_e$. In fact, if the gains are set large enough, the approximation $S_1 + r = \hat{S}_1 + \hat{r}$ is satisfied. See [32] for more details.

Remark 2: The controller parameters $\Lambda, K_1, K_2, K_3, k_o, \tau, \Gamma_1, \Gamma_2, \sigma_1$ and σ_2 may be tuned to adjust the convergence rate λ and the size of ultimate bound ε/λ. The following tuning rules help the user to properly adjust control parameters: (i) considering (53), the larger values of $\Lambda, K_1, K_2, K_3, k_o$ and smaller value of τ increase λ and decrease the size of the ultimate bound ε/λ; (ii) from (61) and (62), larger values of adaptive gains, that is, Γ_1 and Γ_2 increase the convergence rate λ which leads to smaller ultimate bound ε/λ. However, large adaptive gains may result in more robust control actions, which lead to actuators saturation and poor tracking performance; (iii) smaller values of σ_1 and σ_2 decrease the value of ε and consequently leads to smaller ultimate bound ε/λ; (iv) the time functions $\delta(t)$ and $\iota(t)$ in saturation-type controllers f_c and h_c in (28) and (37) may be tuned to compromise between the final tracking accuracy and smoothness of the control signal. The controllers (28) and (37) can be made smoother by choosing a larger value for $\delta(t)$ and $\iota(t)$. However, the larger value of $\delta(t)$ and $\iota(t)$ increases the value of ε in (56) which may result in a larger ultimate bound ε/λ.

Remark 3: In comparison with the previous works [6, 9,12], the proposed control system can overcome the 'explosion of complexity' problem by using the first order filters in the DSC design procedure. This means that the proposed controller does not require the derivative of the virtual controller for the next step in the design procedure. This advantage of DSC technique provides a simpler design than the backstepping approach. This paper has been focused on the design of a simple output feedback control system by using the DSC technique, adaptive robust saturation-type control techniques and a linear observer. Compared to the works of [6,9,12], our proposed control approach has the following advantages: (i) time-consuming and tedious analyses in determining the regression matrices are not required for our proposed controller; (ii) the nonparametric uncertainties such as external disturbances and unmodelled dynamics are completely considered in the design of the proposed controller; (iii) it only designs one virtual controller to compensate for kinematic and dynamic subsystems.

4 SIMULATION RESULTS

In this section, two numerical simulations were performed using MATLAB software to evaluate the tracking performance and robustness of the proposed controller for a fast underactuated surface vessel, which is subjected to both parametric and non-parametric uncertainties. The following ship parameters are chosen to track a desired trajectory based on Look-ahead control method [20]

$$\begin{aligned}&m_{11} = 25.805\,\text{kg}, m_{22} = 33.856\,\text{kg}, m_{33} = 2.743\,\text{kg},\\&d_{11} = 12.436, d_{22} = 17.992\,, d_{33} = 0.564\,.\end{aligned} \tag{66}$$

For simulation purposes, the actuator parameters are chosen as $L_a = diag[0.1, 0.1]\Omega s, R_a = diag[5, 5]\Omega$, $N = diag[48, 48], K_b = diag[0.02, 0.02]^{V}/_{rad/s}, K_T = [0.2, 0.2]$ Nm/A. It is assumed that dynamic parameters and actuators parameters of the vessel are unknown. The non-parametric uncertainties in the vessel and actuators dynamics are simulated by the following signals:

$$\begin{aligned}&\tau_{w2} = [5\sin(t/20), 5\sin(t/20)],\\&u_d = [\sin(t/20), \sin(t/20)].\end{aligned} \tag{67}$$

Moreover, sensor inaccuracies are simulated by zero-mean Gaussian white noise. In the first simulation, the following circular desired trajectory is selected to evaluate the controller performance

$$z_r = [x_f + R\cos(\omega_r t), y_f + R\sin(\omega_r t)], \tag{68}$$

where $(x_f, y_f) = [2.5m, 5.5m], R = 2m$ and $\omega_r = 0.05$ are parameters of the desired trajectory. Remark 2 provide a guideline for the designer to suitably choose control parameters. In our simulations, the following controller parameters achieve a satisfactory tracking performance: $\Lambda = 0.3I_{2\times2}, K_1 = 10.5I_{2\times2}, K_2 = 9I_{2\times2}, K_3 = 4I_{2\times2}, k_o = 20$, $\tau = 0.025$. However, we avoid large control gains to keep the control signals within $|u_i| \leq 24V, i = 1, 2$ in order to prevent actuators saturation. Referring to Remark 2, the adaptive gains are also increased from zero until acceptable adaptation and convergence rates are achieved. The gain values are chosen as $\Gamma_1 = 2diag[1, 1, 0.25, 1]$, $\Gamma_2 = 10^{-3}diag[1, 1, 1, 1]$ and the look ahead distance is chosen as $L = 0.15m$ for the simulation. Other control parameters are set to $\sigma_1 = 0.009, \sigma_2 = 0.00005, \alpha_0 = 0$ and $\beta_0 = 0$. Considering Remark 1, the robust control laws in (28) and (37)

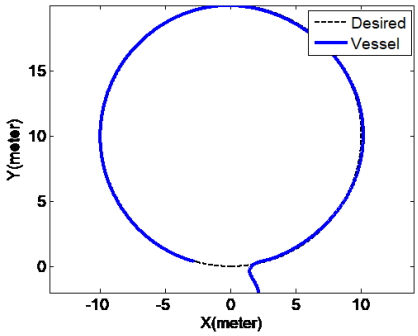

Fig. 3. X–Y plot of desired and the vessel trajectories.

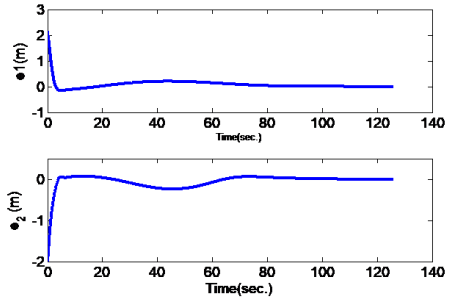

Fig. 4. Output tracking errors.

are selected as

$$f_c(\hat{f}\,\mathrm{sign}(\hat{S}_1+\hat{r})) = \frac{(\hat{S}_1+\hat{r})\hat{f}^2}{\hat{f}\left\|\hat{S}_1+\hat{r}\right\|+\delta(t)}, \qquad (69)$$

$$h_c(\hat{h}\,\mathrm{sign}(S_2)) = \frac{S_2\hat{h}^2}{\hat{h}\,\|S_2\|+\iota(t)}, \qquad (70)$$

which satisfy the conditions (29) and (38). The boundary layer thickness in the control law (69) and (70) is chosen as

$$\delta(t) = \begin{cases} 5000 & if \quad 0 \le t \le 5 \\ 1+e^{-0.2(t-5)} & if \quad t > 5 \end{cases}. \qquad (71)$$

and $\iota(t) = 100$. As stated in remark 2, this choice of $\iota(t)$ reduces high control activities and actuators saturation in the initial time of the trajectory tracking. The initial postures (the position and orientation) of the vessel are set to $[x(0), y(0), \psi(0)] = [6, 5, \pi/7]$ for this simulation.

Fig. 3 shows the x–y plot of desired and actual trajectories of the vessel. The output tracking errors are also shown by Fig. 4. From the figures, the robustness and tracking response of the proposed controller is desirable despite structured and unstructured uncertainties. Linear and angular velocities estimation are shown in Fig. 5, Fig.

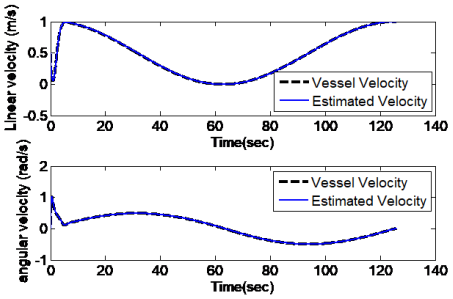

Fig. 5. Linear and angular velocities and their estimations.

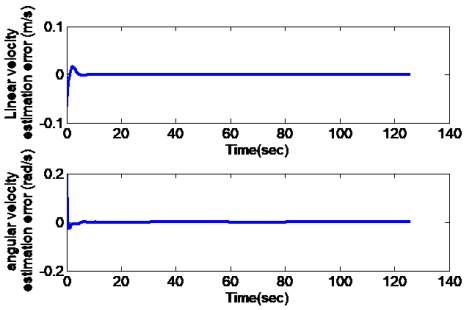

Fig. 6. Linear and angular velocities estimation errors.

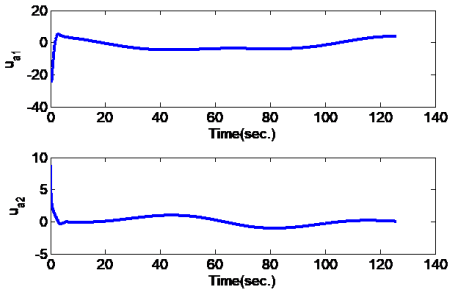

Fig. 7. Generated control signals.

6 demonstrates the linear and angular velocities estimation errors. Figs. 4 and 5 show that the output tracking errors $z_e = z - z_d$ and velocity estimation errors converge to a small compact set. Figs. 7 shows the generated control signals which are fed to the vessel actuators. The estimates of unknown parameters of the upper-bounding functions in the vessel model and actuators dynamics are illustrated by Figs. 8 and 9. As it can be seen from the figures, the parameter estimates are also bounded. The user may adjust the size of the ultimate bound $\varepsilon(t)$, convergence rate λ and smoothness of the control signals by adjusting control parameters $K_1, K_2, K_3, \Gamma_1, \Gamma_2, \alpha_0, \beta_0, \sigma_1, \sigma_2, \delta_1(t), \rho(t)$.

Then, a flower-shaped desired trajectory is chosen to assess the controller performance in the following simula-

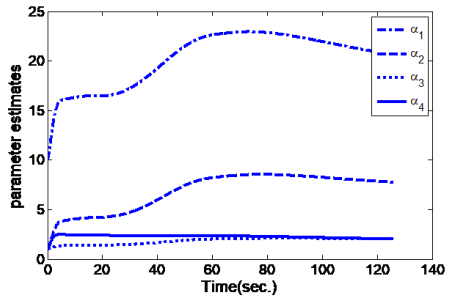

Fig. 8. Estimated parameters of the upper-bounding functions for uncertain non-linearities.

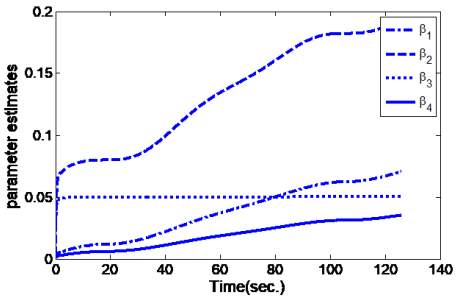

Fig. 9. Estimated parameters of the upper-bounding functions for uncertain non-linearities.

tion. For this purpose, the desired trajectory is given by

$$z_r = \begin{array}{l}[x_f + R\sin(2\omega_r t) + R\cos(\omega_r t),\\ y_f + R\sin(\omega_r t) + R\cos(2\omega_r t)]\,.\end{array} \quad (72)$$

The following controller parameters achieve a satisfactory tracking performance: $\Lambda = 1.2I_{2\times 2}, K_3 = 3I_{2\times 2}$ and other parameters are selected as same as the first simulation. The initial postures of the vessel are set to $[x(0), y(0), \psi(0)] = [2.5, 9.5, pi/6]$ for this simulation. Fig. 10 to Fig. 16 show the tracking results of the proposed controller for the desired trajectory (72). To show the noisy position measurements, a close-up of Fig. 10 is shown in Fig. 17. As stated before, large control gains may be cause actuators saturation and as a result degrade the performance of the controller. Fig. 18 illustrates the x–y plot of desired and actual trajectories of the vessel when large control gains are chosen. From the figures, it can be seen that the tracking performance and robustness of the output feedback controller are desirable. Therefore the presented simulation results verify that our proposed controller is effective to solve the trajectory tracking problem of an underactuated fast surface vessel without velocity measurements.

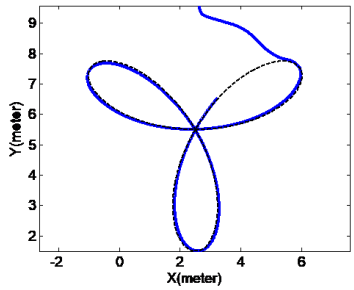

Fig. 10. X–Y plot of desired and the vessel trajectories.

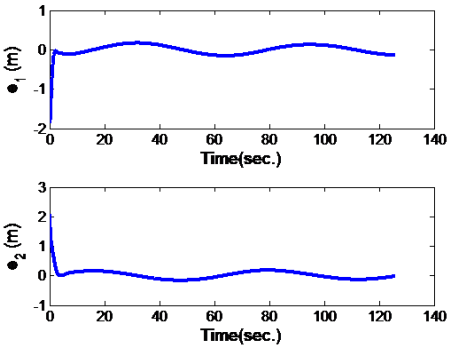

Fig. 11. Output tracking errors.

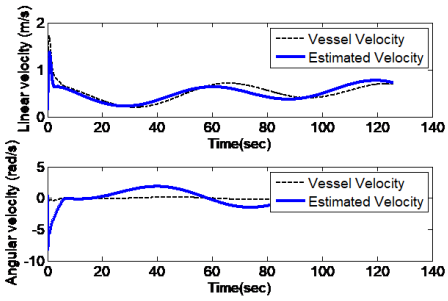

Fig. 12. Linear and angular velocities and their estimationsvessel.

4.1 Comparative study

Here, our aim is to show the efficacy of the proposed control approach compared with the previous output feedback control system in [24]. It is shown that, their proposed output feedback controller shows a satisfactory tracking performance in the presence of parametric uncertainties. In practice, the surface vessel and actuators dynamics are also subjected to non-parametric uncertainties. Such uncertainties may be caused by unmodelled dynamics of the system. As mentioned before, the proposed controller in [24] does not take non-parametric uncertainties into account, which may lead to a poor tracking performance. By adopting the

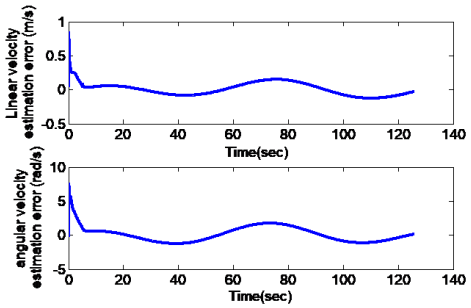

Fig. 13. Linear and angular velocities estimation errors.

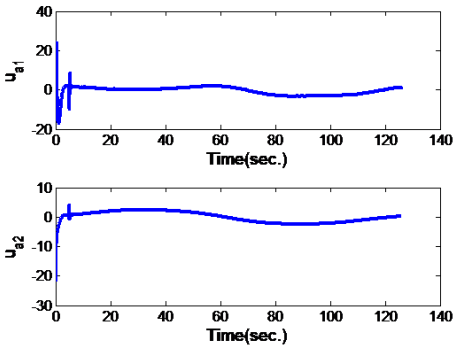

Fig. 14. Generated control signals by the proposed controller.

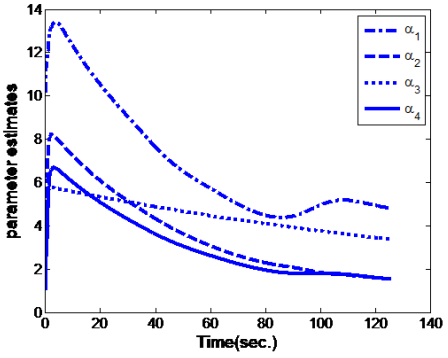

Fig. 15. Estimated parameters of the upper-bounding functions for uncertain non-linearities.

presented models, simulation parameters in [24], another computer simulation has been performed for a comparative study. The simulation results are illustrated by Figs. 19 and 20 to compare the tracking performance and robustness of our proposed controller with the proposed controller in [24]. The uncertainties are assumed as (67). From Figs. 19 and 20, the robustness and the tracking response of the controller, which is proposed in [24], is not acceptable due to a large amount of unstructured uncertainties.

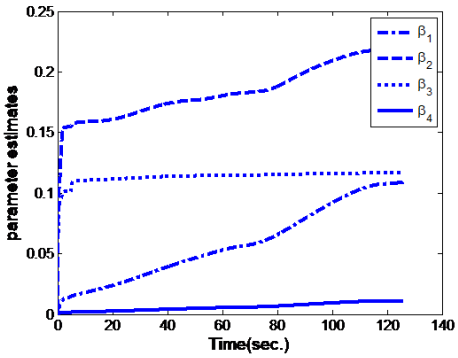

Fig. 16. Estimated parameters of the upper-bounding functions for uncertain non-linearities.

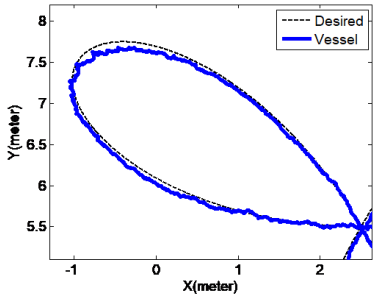

Fig. 17. Noisy position measurements.

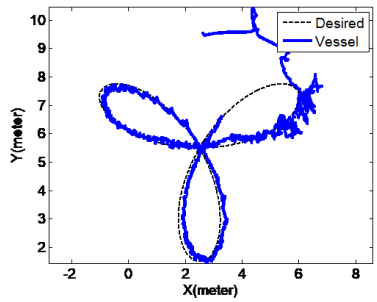

Fig. 18. X–Y plot of desired and the vessel trajectories when actuators saturation occurs.

However, as shown in Figs. 3 and 4 our proposed control system successfully tracks the desired trajectory by taking the advantage of an adaptive robust saturation-type controller.

5 CONCLUSION

In this paper, the problem of the adaptive robust observer-based controller has been addressed for an underactuated fast surface vessel including actuator dynamics by considering both parametric and nonparametric uncertainties. At

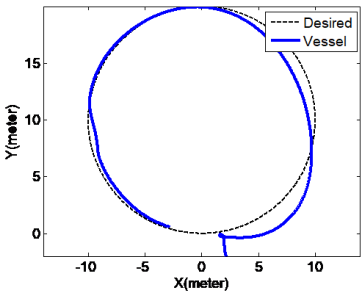

Fig. 19. X–Y plot of desired and the vessel trajectories in [24].

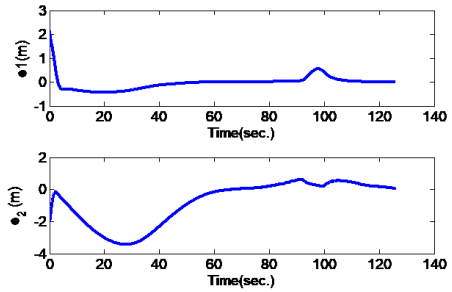

Fig. 20. Output tracking errors in [24].

first, one virtual controller was only designed at the kinematic and dynamic levels and a linear observer is used to estimate the velocity vector. Next, the DSC method has been used to design the tracking control law for the actuator dynamics without the time derivative of the virtual control law. A Lyapuonv-based stability analysis was provided to prove that the tracking and state estimation errors are UUB and the corresponding ultimate bound can be adjusted by control parameters. To compare with the proposed controller, an adaptive output tracking controller was simulated. Simulation results were demonstrated proposed controller successfully tracks the desired trajectory by taking the advantage of an adaptive robust saturation-type controller

APPENDIX A

Differentiating (51) along (25), (26), (45), (47), (49), (30) and (39) and considering that $\dot{\tilde{\alpha}} = -\dot{\hat{\alpha}}$ and $\dot{\tilde{\beta}} = -\dot{\hat{\beta}}$ yield

$$\begin{aligned}\dot{V}(t)=&z_e^T K_2 \dot{z}_e + z_z^T K_2 \dot{z}_z + S_1^T M_2(\psi)\dot{S}_1 + \frac{1}{2}S_1^T \dot{M}_2(\psi) S_1 \\ &+ r^T M_2(\psi)\dot{r} + \frac{1}{2} r^T \dot{M}_2 r + S_2^T L_a \dot{S}_2 + e_f^T \dot{e}_f \\ &- \tilde{\alpha}\Gamma_1^{-1}\dot{\hat{\alpha}} - \tilde{\beta}^T \Gamma_2^{-1}\dot{\hat{\beta}}\end{aligned}$$

$$\begin{aligned}\dot{V}(t)=&z_e^T K_2 S_1 - z_e^T K_2 \Lambda z_e + z_e^T K_2 \Lambda z_z + z_z^T K_2 r \\ &- z_z^T K_2 \Lambda z_z - S_1^T C_2(v,\psi,\dot{z}) S_1 + S_1^T \chi_1 + S_1^T \xi \\ &+ S_1^T J^{-T}(\psi)(e_f + S_2) - S_1^T K_1 S_1 + S_1^T K_1 r \\ &- S_1^T K_2 z_e - S_1^T K_2 z_z - S_1^T f_c + \frac{1}{2} S_1^T \dot{M}_2(\psi) S_1 \\ &- r^T C_2(v,\psi,\dot{z}) r + r^T \chi_2 - r^T (k_o M_2(\psi) - K_1) r \\ &- r^T K_1 S_1 - r^T K_2 z_e + r^T \xi - r^T K_2 z_z \\ &+ r^T J^{-T}(\psi)(e_f + S_2) - r^T f_c + \frac{1}{2} r^T \dot{M}_2(\psi) r \\ &- S_2^T K_3 S_2 - S_2^T R_a S_2 - S_2^T h_c - S_2^T N K_b X J^{-1} S_1 \\ &+ S_2^T N K_b X J^{-1} \Lambda z_e - S_2^T N K_b X J^{-1} \Lambda z_z \\ &+ S_2^T \zeta + e_f^T \dot{e}_f - \tilde{\alpha}^T F^T \|S_1 + r\| \\ &+ \tilde{\alpha}^T \sigma_1(\tilde{\alpha} - \alpha_0) - \tilde{\beta}^T H^T \|S_2\| + \tilde{\beta}^T \sigma_2(\tilde{\beta} - \beta_0)\end{aligned} \tag{73}$$

Considering property 4, the inequality (73) can be rewritten as

$$\begin{aligned}\dot{V}(t) \leq &- z_e^T K_2 \Lambda z_e - z_z^T K_2 \Lambda z_z - S_1^T K_1 S_1 \\ &- r^T (k_o M_2(\psi) - K_1) r - S_2^T K_3 S_2 - S_2^T R_a S_2 \\ &+ (S_1 + r)^T (\xi - f_c) + S_2^T (\zeta - h_c) + \left\|S_1^T\right\| \|\chi_1\| \\ &+ \left\|r^T\right\| \|\chi_2\| + \|S_1\| \left\|J^{-T}\right\| \|e_f\| + \|S_1\| \left\|J^{-T}\right\| \|S_2\| \\ &+ \|S_1\| \|K_2\| \|z_z\| + \|K_2 \Lambda\| \|z_e\| \|z_z\| + \|r\| \|K_2\| \|z_e\| \\ &+ \|r\| \left\|J^{-T}\right\| \|e_f\| + \|r\| \left\|J^{-T}\right\| \|S_2\| + \|S_2\| \times \\ &\left\|N K_b X J^{-1}\right\| \|S_1\| + \|S_2\| \left\|N K_b X J^{-1} \Lambda\right\| \|z_e\| \\ &+ \|S_2\| \left\|N K_b X J^{-1} \Lambda\right\| \|z_z\| - \tilde{\alpha}^T F^T \|S_1 + r\| + e_f^T \dot{e}_f \\ &+ \tilde{\alpha}^T \sigma_1(\hat{\alpha} - \alpha_0) - \tilde{\beta}^T H^T \|S_2\| + \tilde{\beta}^T \sigma_2(\hat{\beta} - \beta_0).\end{aligned} \tag{74}$$

Since for any $P_1 > 0$ and $P_2 > 0$, the following sets

$$\begin{aligned}\prod\nolimits_1 = \{\ &(z_d, \dot{z}_d, \ddot{z}_d, \dddot{z}_d) : \\ &z_d^T z_d + \dot{z}_d^T \dot{z}_d + \ddot{z}_d^T \ddot{z}_d + \dddot{z}_d^T \dddot{z}_d \leq P_1\ \}.\end{aligned} \tag{75}$$

$$\prod\nolimits_2 = \{\ (S_1, S_2, z_e, z_z, r, e_f, \tilde{\alpha}, \tilde{\beta}) : \quad V(t) \leq P_2\ \}. \tag{76}$$

are compact in $\Re^8$ and $\Re^{20}$, respectively, $\prod_1 \times \prod_2$ is also a compact set in $\Re^{28}$. Thus, ρ in (42) has a maximum value ρ_m in $\prod_1 \times \prod_2$, that is $\rho \leq \rho_m$. By considering this fact and recalling inequality (44), and considering the following facts

$$\|K\| \|x_1\| \|x_2\| \leq \frac{1}{2}\|K\| x_1^T x_1 + \frac{1}{2} \|K\| x_2^T x_2, \forall x_1, x_2 \in \Re^n. \tag{77}$$

The inequality (76) is rewritten as (52).

[1] A. P., Aguiar, J. P., Hespanah, "Trajectory tracking and path-following of underactuated autonomous vehicles with parametric modeling uncertainty", IEEE Transaction on Automatic Control, Vol. 52, pp. 1362–1379, 2007.

[2] K. Y. Pettersen, "Exponential Stabilization of Underactuated Vehicles", Ph.D. thesis, Norwegian University of Science Technology, Trondheim, Norway, 1996

[3] R. W., Brockett, "Asymptotic stability and feedback linearization," in Differential Geometric Control Theory, R.W. Brockett, R. S. Millman, and H. J. Sussman, Eds. Boston, MA: Birkhauser, pp. 181–191, 1983.

[4] K. D., Do, J., Pan, "State and output-feedback robust path-following controllers for underactuated ships using Serret–Frenet frame", Ocean Engineering, Vol. 11, pp. 587–613, 2004.

[5] J., Ruan, Z., Li, F., Zhou, Y., Li, "ADRC based ship tracking controller design and simulations", IEEE International Conference on Automation and Logistics, pp. 1763–1768, 2008.

[6] Z. P., Jiang, "Global tracking control of underactuated ships by Lyaounov's direct method", Automatica, Vol. 38, pp. 301–309, 2002.

[7] L. P., Perera, C. G., Soares, "Pre-filtered sliding mode control for nonlinear ship steering associated with disturbances", Ocean Engineering, Vol. 51, pp. 49–62, 2012.

[8] S., Oh, J., Sun, "Path following of underactuated marine surface vessels using line-of-sight based model predictive control", Ocean Engineering, Vol. 37, pp. 289–295, 2010.

[9] K. D., Do, Z. P., Jiang, J., Pan, "Robust global stabilization of underactuated ships on a linear course: state and output feedback", International Journal of Control, Vol. 76, pp. 1–17, 2003.

[10] K. D. Do, J., Pan, "Global tracking control of underactuated ships with nonzero off-diagonal terms in their system matrices", Automatica, Vol. 41, pp. 87–95, 2005.

[11] Z., Li, J., Sun, S., Oh, " Design, analysis and experimental validation of a robust nonlinear path following controller for marine surface vessels", Automatica, Vol. 45, pp. 1649–1658, 2009.

[12] J., Ghommam, F., Mnif, N., Derbel, "Global stabilisation and tracking control of underactuated surface vessels", IET Control Theory and Applications, Vol. 4, pp. 71–88, 2008.

[13] H., Ashrafiuon, K. R., Muske, L. C., McNinch, R. A., Soltan, "Sliding mode tracking control of surface vessels", IEEE Transactions on Industrial Electronics, Vol.55, pp. 4004–4012, 2008.

[14] K. D., Do, J., Pan, "Control of ships and underwater vehicles", New York, NY, USA: Springer-Verlag, 2009.

[15] K. D. Do, J. Pan, "Robust path-following of the underactuated ships: Theory and experiments on a model ship", Ocean Engineering, Vol. 33, pp. 1354–1372, 2006.

[16] K. D. Do, Z. P. Jiang, J. Pan, "Global robust adaptive path-following of underactuated ships", Automatica, Vol. 42, pp. 1713–1722, 2006.

[17] H., Katayama, H., Aoki, "Sampled-data straight-line path following control for underactuated ships", 50th IEEE Conference on Decsion and Control and European Control Conference, pp. 3946–3951, 2011.

[18] M., Movahed, S., Dadashi, M., Danesh, "Adaptive Sliding Mode Control for Autonomous Surface Vessel", In Proceedings of the 2011 IEEE International Conference on Mechatronic, pp. 522–527, 2011.

[19] R., Yu, Q., Zhu, G., Xia, Z., Liu, "Sliding mode tracking control of an underactuated surface vessel", IET Control Theory App, Vol. 6, pp. 461–466, 2011.

[20] K. D., Do, J., Pan, "Underactuated ships follow smooth paths with integral actions and without velocity measurements for feedback: Theory and experiments", IEEE Transactions on Control Systems Technology, Vol. 14, pp. 308–322, 2006.

[21] K. D., Do, "Practical control of underactuated ships", Ocean Engineering, Vol. 37, pp. 1111–1119, 2010.

[22] C. Dongkyoung, "Global tracking control of underactuated ships with input and velocity constraints using dynamic surface control method", IEEE Transaction on Control Systems Technology, Vol. 19, pp. 1357–1370, 2011.

[23] K. D., Do, Z. P., Jiang, J., Pan, "Global partial-state feedback and output-feedback tracking controllers for underactuated ships", Systems and Control Letters, pp. 1015–1036, 2005.

[24] D., Lee, E., Tatlicioglu, T.C., Burg, D.M., Dawson, "Adaptive output tracking control of a surface vessel", In the Proceedings of the 47th IEEE Conference on Decision and Control, pp. 1352– 1357, 2008.

[25] H., Katayama, H., Aoki, " Straight-Line Trajectory Tracking Control for Sampled-data underactuated ships", IEEE Transactions on control systems technology, pp. 1–8, 2013.

[26] D., Swaroop, J.K., Hedrick, P.P., Yip, "Dynamic surface control for a class of nonlinear systems", IEEE Transaction on Automatic Control, Vol. 45, pp. 1893–1899, 2000.

[27] K., Shojaei, A. M., Shahri, "Output feedback tracking control of uncertain non-holonomic wheeled mobile robots: a dynamic surface control approach", IET Control Theory Appl., Vol. 6, pp. 216–228, 2011.

[28] H. K., Khalil, "Nonlinear systems", Prentice-Hall, Upper Saddle River, NJ, 1996.

[29] T. I. Fossen, "Marine Control Systems", Trondheim, Norway: Marine Cybernetics, 2002

[30] J. H., Li, P. M., Lee, B. H., Jun, Y.K., Lim, "Point-to-point navigation of underactuated ships", Automatica, Vol. 44, pp. 3201–3205, 2008.

[31] B., Yao, "Adaptive robust control of nonlinear systems with application to control of mechanical systems," PhD thesis, University of California, 1996.

[32] M. A., Arteaga, R., Kelly, "Robot control without velocity measurements: new theory and experimental results", IEEE Transaction on Robotics and Automation, Vol. 20, pp. 297–308, 2004.

[33] Z., Qu, D. M., Dawson, "Robust tracking control of robot manipulators", EEE Press, Piscataway, NJ, 1996.

[34] Karlsen, A.T., "On Modeling of a Ship Propulsion System for Control Purposes", Institut for teknisk kybernetik, 2012.

Padideh Rasouli received her B.S-degree and M.S-degree in electrical engineering from Najafabad Branch, Islamic Azad University, Iran in 2008 and 2013, respectively. Currently, she is pursuing her Ph.D. from Marvdasht Branch, Islamic Azad University, Iran. Her main research interests are the control of nonlinear and robotic systems and bilateral teleoperation over the Internet.

Khoshnam Shojaei was born in Esfahan, Iran, on March 8, 1981. He received his B.S-degree, MS-degree, and Ph.D.-degree with distinction in electrical engineering from Iran University of Science and Technology (IUST) in 2004, 2007 and 2011, respectively. Currently, he is an assistant professor in Najafabad Branch, Islamic Azad University, Iran. His research areas are adaptive control of nonlinear systems, control of autonomous robots including land, air and ocean vehicles, and navigation of mobile robots.

Abbas Chatraei received his M.S. degrees in electrical engineering from Islamic Azad University, Najafabad branch, Iran in 2002. In 2011, he received his Ph.D. degree in the field of "Optimal control of industrial robots" in Faculty of Mechatronics, Informatics and Interdisciplinary Studies of Technical University of Liberec (TUL) (in Czech Republic). His research interests are in the areas of robot's nonlinear control and system identification. At present, he is an assistant professor at department of electrical engineering, Najafabad Branch, Islamic Azad University, Iran.

AUTHORS' ADDRESSES

Padideh Rasouli
Khoshnam Shojaei, Ph.D, Assistant Professor
Abbas Chatraei, Ph.D, Assistant Professor

Affiliation: Department of Electrical Engineering, Najafabad Branch, Islamic Azad University, Najafabad, Iran

Address: Daneshgah Boulevard, Najafabad, Isfahan 8514143131, Iran
phone: +98 31 4229 24 58
email: khoshnam.shojaee@gmail.com; shojaei@pel.iaun.ac.ir

Corresponding Author: Khoshnam Shojaei

Received: 2015-09-23
Accepted: 2017-09-29